Karlsruher Institut für Technologie

Global Logistics of an Iron-based Energy Network: A Case Study of Retrofitting German Coal Power Plants

Erik Jansen, Julia Schuler, Armin Ardone, Viktor Slednev, Wolf Fichtner and Marc E. Pfetsch

No. 70 | APRIL 2023

WORKING PAPER SERIES IN PRODUCTION AND ENERGY

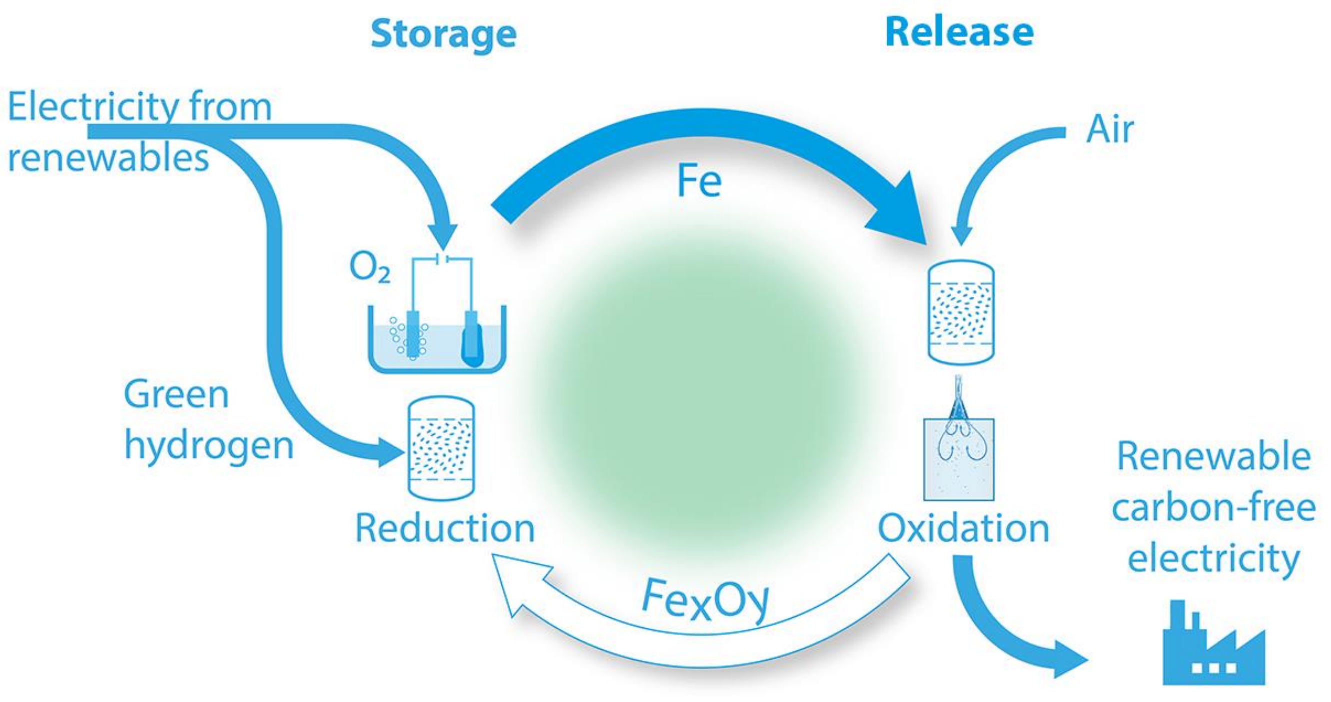

Global Logistics of an Iron-based Energy Network: A Case Study of Retrofitting German Coal Power Plants

Erik Jansen[1], Julia Schuler[2], Armin Ardone[2], Viktor Slednev[2], Wolf Fichtner[2] and Marc E. Pfetsch[1]

[1]Technical University of Darmstadt, Department of Mathematics, RG Discrete Optimization, Dolivostraße 15, 64293 Darmstadt, Germany

[2]Karlsruhe Institute of Technology, Institute for Industrial Production, Chair of Energy Economics, Hertzstraße 16, 76187 Karlsruhe, Germany

jansen@mathematik.tu-darmstadt.de
julia.schuler@kit.edu

Abstract

For the global transition of energy systems, the establishment of new energy storage and carrier media to balance the geographical and temporal availability of renewable energy is a necessity. In this context, the interdisciplinary cluster project Clean Circles is investigating the potential of an iron-based circular energy economy. Compared to hydrogen, an energy carrier produced from renewables through electrolysis and widely discussed option for future global energy trade, iron offers several advantages. An iron-based circular energy economy re-uses existing infrastructure associated with the transportation of and the electricity generation from coal. In this paper, we present a model-based approach for the cost-minimal selection of energy export regions and logistic routes to import iron for electricity generation to power plant sites in Germany and return iron oxide to reduction plants in the export regions. To demonstrate the performance of the model, we conduct a case study of operating all German hard coal-fired power plants in operation in 2030 on iron. For the iron reduction process site selection, we provide the optimization with renewable energy potentials and costs in coastal regions of MENA and Patagonia.

Global Logistics of an Iron-based Energy Network: A Case Study of Retrofitting German Coal Power Plants

Erik Jansen[1], Julia Schuler[2], Armin Ardone[2], Viktor Slednev[2], Wolf Fichtner[2] and Marc E. Pfetsch[1]

[1] *Technical University of Darmstadt, Department of Mathematics, RG Discrete Optimization, Dolivostraße 15, 64293 Darmstadt, Germany*

[2] *Karlsruhe Institute of Technology, Department of Economics and Management, Institute for Industrial Production, Chair of Energy Economics, Hertzstraße 16, 76187 Karlsruhe, Germany*

April 27, 2023

Abstract

For the global transition of energy systems, the establishment of new energy storage and carrier media to balance the geographical and temporal availability of renewable energy is a necessity. In this context, the interdisciplinary cluster project *Clean Circles* is investigating the potential of an iron-based circular energy economy. Compared to hydrogen, an energy carrier produced from renewables through electrolysis and widely discussed option for future global energy trade, iron offers several advantages. An iron-based circular energy economy re-uses existing infrastructure associated with the transportation of and the electricity generation from coal. In this paper, we present a model-based approach for the cost-minimal selection of energy export regions and logistic routes to import iron for electricity generation to power plant sites in Germany and return iron oxide to reduction plants in the export regions. To demonstrate the performance of the model, we conduct a case study of operating all German hard coal-fired power plants in operation in 2030 on iron. For the iron reduction process site selection, we provide the optimization with renewable energy potentials and costs in coastal regions of MENA and Patagonia.

Acknowledgements

This work was performed within the cluster project Clean Circles. Funding by the Hessian Ministry of Higher Education, Research, Science and the Arts as well as the Strategy Fund of the KIT Presidium is gratefully acknowledged.

1 Introduction

With the transition of energy systems from fossil fuels to renewable energies (RES), the challenge of spatial separation of energy demand and supply remains. Volatile RES generation profiles create an additional complexity. Consequently, many countries will continue to depend on energy imports in the future. In the case of Germany, achieving climate neutrality in 2045 is expected to require an import share of more than 40 % of primary energy demand [1]. Hence, a crucial challenge regarding the future energy system lies in the establishment of new energy storage and carrier media to balance geographical and temporal availability of renewable energy. To facilitate trading, the new energy carriers should be comparable to oil, coal, and gas in terms of price, energy content or handling.

While hydrogen is currently the most prominent candidate, research indicates that reactive metals are also a highly promising option. Several metals can be combusted similarly to fossil fuels, however, because the combustion products are solid, the corresponding metal oxides can be captured and recycled in a reduction process. The metals are zero-carbon energy carriers when both transportation and reduction are RES-based (for example, reduction with hydrogen produced by RES-driven water electrolysis). The most important characteristics that support metals as energy carriers complementary to hydrogen are very high volumetric energy densities, low costs, almost loss-free long-term storage and transport under atmospheric conditions as well as promising energy cycle efficiencies [2, 3]. Meanwhile, hydrogen transport is not yet available on industrial scale and presents challenges. They also allow for the ongoing use of existing infrastructure, such as ships, rail and trucks used for bulk material transportation. Research indicates that coal-fired power plants could be operated with iron after some (minor) modifications [4]. Reactive metals have the potential to be used for import of energy from RES-rich regions as well as to store domestic excess RES generation.

The interdisciplinary German cluster project *Clean Circles*, to which our work contributes, is investigating the potential use of iron as an energy carrier [5]. Iron is the fourth most abundant element in the earth crust, cheap, non-toxic, and has oxidation flame temperatures similar to those of hydrocarbons. Compared to liquefied hydrogen, iron powder has a volumetric energy density that is nearly three times higher. The carbon free iron-based energy cycle is depicted in Figure 1. Previous publications within the project focus on high-temperature oxidation of single iron particles [6], infrastructure requirements to retrofit coal power plants for iron combustion [7] and techno-economic comparison of iron to hydrogen, natural gas and coal [8]. Complementary, this paper proposes a modeling approach for coupled optimization of iron logistics and iron reduction process site selection.

Our objective is the determination of the cost-minimal combination of export regions and logistic routes to import a certain amount of iron for electricity generation to specific power plant sites and return iron oxide to reduction plants, using dry bulk carriers for overseas and barges or trains for inland transport. For this purpose, a logistic network combined with an optimization problem where designed.

To demonstrate the model's functionality, we apply it to a scenario in which all German hard coal-fired power plants in operation in the target year 2030 generate electricity based on iron. For the iron reduction site selection, the model is provided with information about capacities, coordinates and costs of potential renewable energy parks in coastal regions of 16 countries in the MENA region and Patagonia. Electricity generation costs at the power plants are calculated under neglection of investment costs in transportation, as the re-use of existing coal infrastructure is assumed. Moreover, because there are no reliable cost estimates yet (but

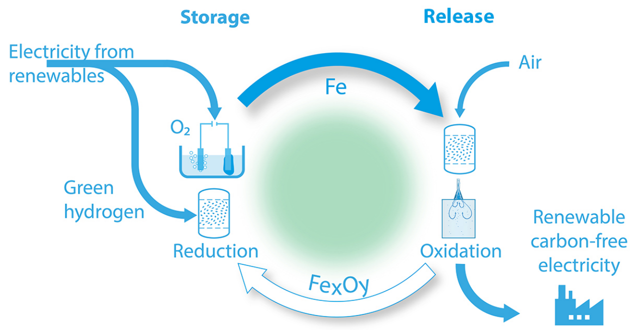

Figure 1: Iron cycle process scheme

first studies indicate that the costs are minor [4]), the costs for retrofitting existing coal-fired power plants are not taken into consideration. The supply chains are optimized regarding costs. Furthermore, analyses of their efficiencies and CO_2-emissions are conducted. These results are compared to coal-fired electricity generation by determining the break-even CO_2-price at which iron is competitive.
Our methods are not limited to this scenario, as other countries could be examined both on the supply as well as on the demand site, and the model could easily be adapted to other (circular) energy supply chains.
The paper is structured as follows: The underlying methodology is explained in the following Section 2. Section 3 contains the case study data, while Section 4 has the corresponding results. We conclude with a discussion of the model in Section 5.

2 Network Design Problem

In the following we describe the abstract formulation of our network design problem, a network model combined with a hereon operating optimization problem. This model is then employed to perform the case study using data and supplementary model equations to describe components and processes of the iron cycle provided in Section 3.

2.1 Network Structure

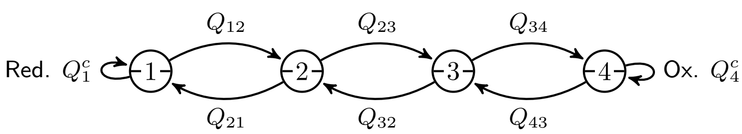

Figure 2: Scheme of the levels of the logistic cycle ($Q_{\cdot}$: Flow Quantity)

The network is structured in levels, with four nodes representing key stations along the energy supply chain and interconnecting edges as illustrated in Figure 2. We only allow transportation between consecutive levels. Both directions are feasible between consecutive levels, as both the transportation of iron from renewable energy-rich exporting regions to Germany as well as the

reverse transportation of iron oxide is depicted to model the closed iron cycle. Outward and return routes are not specifically chosen to be symmetric but the optimization leads to such in the majority of cases.
The first level are solar and wind parks. The second level consists of sea ports of the exporting regions, the third level of intermediate transshipment ports in Europe, and the last level of the retrofitted hard coal power plants in Germany. To respect different transport routes and modes, multiple edges between two nodes can be implemented. In the current model, this is only realized between Level 3 and 4 to allow inland transport in Germany via trains or waterways. The iron reduction and oxidation processes are represented as self-loops (Q^c) at the nodes in Level 1 and 4.
We only consider one circulation of material in the network. Hence, the need for reduced iron has to be fulfilled with one import cycle. Limitations are not taken into account along the edges (routes) of the energy supply chain, only the capacities of nodes (locations) are limiting factors in the network. Throughout the network, we describe the flow by Mt of transported/converted material. The material needs to pass each level before returning. This is ensured by separated mass flow conversion and corresponding flow constraints as part of the optimization problem presented in the following section.

2.2 Optimization Problem

Based on the described network, an optimization problem is implemented to identify the cost-minimal configuration from sets of possible locations per level and routes to fulfill a given demand of iron at the last level. The parameters, optimization variables, sets of nodes and edges as well as objective function of this optimization problem are described in the following.

Parameters

V all nodes of the network

L_i all nodes in level i of the network

E all edges (backwards and forwards) of the network

cap_u iron reduction capacity at node u

dem_u iron demand at node u

c_{uv} variable costs per transported Mt from node u to node v

c_u variable costs per processed Mt at node u

f_u fixed cost for using node u

Variables

Q_{uv} quantity in Mt of material transported from node u to node v (material clear by direction)

Q_u^c quantity in Mt of material converted in node u in L_1 or L_4 (process clear by location)

W_u binary variable that equals 1 if a node $u \in V$ is used and operating, 0 otherwise

The respective parameter values for the case study are discussed and derived in Section 3.
The objective of the optimization is the minimization of costs of the overall network. Costs consist of variable costs over nodes/self-loops c_u and edges c_{uv} as well as fixed costs per node f_u.
Variables of the optimization are the selection of suppliers and ports W_u as well as the choice of routes and amount of transported/converted goods within the network Q_{uv}/Q^c_u. Iron demands dem_u and iron reduction capacities cap_u are crucial parameters determining the needed amount of iron in the network and the eligibility of export regions.
The change in weight by oxidation/reduction (43 % increase/decrease) is considered via a manipulation of the conservation of mass constraints at the respective plants via self-loops in Level 1 and 4, cf. Figure 2. Each flow over the loops Q^c represents the actual weight of the to-be-transformed material. The flow variable is denoted as mass in Mt. $\delta^{\pm}(u)$ describes the set of all incoming and outgoing edges, while $\delta(u)$ is the set of all adjacent edges. The optimization problem with objective function and constraints can be summarized as follows:

$$\min_{\substack{Q_{uv},Q^p_u\in\mathbb{R}_+,\\ W_u\in\{0,1\}}} \sum_{(u,v)\in E} c_{uv}\cdot Q_{uv} + \sum_{u\in V} f_u\cdot W_u + \sum_{\substack{u\in V,\\ v\in\delta^+(u)}} c_u\cdot Q_{uv} + \sum_{u\in L_1\cup L_4} c_u\cdot Q^c_u$$

$$\begin{aligned}
\text{Capacity:}\quad & Q^c_u \le cap_u\cdot W_u, && \forall u\in L_1\\
& Q^c_u \le cap_u, && \forall u\in L_4\\
\text{Demand:}\quad & Q^c_u \ge dem_u, && \forall u\in L_4\\
& Q^c_u \ge 0.02\cdot dem_u\cdot W_u, && \forall u\in L_1\\
\text{Flow:}\quad & \sum_{v\in\delta^-(u)} Q_{vu} = Q^c_u, && \forall u\in L_1\\
& \tfrac{1}{1.43}\cdot Q^c_u = \sum_{v\in\delta^+(u)} Q_{uv}, && \forall u\in L_1\\
& \sum_{v\in\delta^-(u)} Q_{vu} = \sum_{v\in\delta^+(u)} Q_{uv}, && \forall u\in V\setminus\{L_1\cup L_4\}\\
& \sum_{v\in\delta^-(u)} Q_{vu} = Q^c_u, && \forall u\in L_4\\
& 1.43\cdot Q^c_u = \sum_{v\in\delta^+(u)} Q_{uv}, && \forall u\in L_4\\
\text{Selection:}\quad & (1-2\cdot W_u)\cdot\sum_{v\in\delta(u)} Q_{uv} \le 0, && \forall u\in L_2\cup L_3.
\end{aligned}$$

In the objective function, the first term describes variable costs over the network edges like transport, canal and, if considered, emission costs. The second term comprises either fixed costs for using the corresponding node. In this case study we only consider fixed operational costs. Potentially, fixed costs for constructing or retrofitting infrastructure could also be considered here in a further development of the model. The last constraint ensures that these fixed costs are getting correctly calculated by setting each node with any flow-through as 1.

The third term describes variable cost per node such as processing costs or port fees. The fourth term is used for costs at self-loops on level 1 and 4. For the conversion costs at the first nodes of the network L_1, we developed a method for quantifying iron reduction costs (see Section 3.1). This allows to compare iron supply costs to other energy carriers. For the oxidation site L_4, we consider variable power plant operational costs as conversion costs at the nodes.
We solve the resulting mixed-integer linear problem (MILP) with the SCIP Optimization Suite [9] on an Ubuntu computer with eight kernels with 3.4 GHz and 16 GB RAM storage in 5 second.

3 Assumptions and Data related to the Case Study

All values and assumptions to adopt the optimization model to the case study are listed below along with their literature reference, divided into the sections "Export Regions", "Transport" and "Import Country". Wherever possible, the year 2030 serves as the time horizon for the parameters. If other reference years are used for costs, they are adjusted for inflation to 2030 based on the HICP index. For historic data we use [10], for data up to 2025 the prognosis of the european central bank [11] and after 2025 the postulated target of the European Central Bank of 2 % inflation [12]. While all costs are inflation-adjusted to the target year 2030, as we use cost estimates from different sources, the base years for price projections vary or are sometimes not available. For LCOE from exporting regions, cost projections for the year 2030 are with respect to the base year 2020.

3.1 Export Regions

Transport distance on the one hand and local iron supply costs and capacities on the other are crucial parameters for the model's choice of iron reduction locations in Patagonia and the MENA region. Since electricity is required for hydrogen production via electrolysis, for intermediate high-pressure hydrogen storage and for the iron reduction process, the site-specific costs of iron reduction are greatly influenced by local costs of renewable electricity.

Renewable energy potentials in MENA states and Patagonia
The optimization selects the most suitable locations for the iron reduction process in the MENA region and Patagonia. Those regions were chosen to compare high-potential regions with a broad range of transport distances to Germany. We provide the estimated renewable energy potentials of coastal areas up to 50 kilometers from the nearest of 61 existing seaports in MENA and Patagonia in the following 16 countries: Israel, Egypt, Jordan, Saudi Arabia, Oman, United Arab Emirates, Qatar, Kuwait, Iraq, Libya, Tunisia, Algeria, Western Sahara, Morocco, Argentina and Chile.
Input parameters include local RES expansion potential, electricity generation costs and hourly generation time series for offshore and onshore wind power turbines, photovoltaic and solarthermal generation. Individual plants are clustered to form 1 029 solar and wind farms with a total potential generation capacity of 3 340 GW. Average electricity generation costs are 20.07 €/MWh, derived from investment costs in the range of 392 €/kW to 4 103 €/kW and fixed operational costs ranging from 2.59 €/kW to 53.6 €/kW per year. Cheapest electricity generation is assumed at a potential 1 172 MW onshore wind farm in Western Sahara with

7.6 €/MWh at a high annual utilization rate of 61 %, with investment costs of 716 €/kW and operational costs of 12.7 €/kW per year.
The calculation of the renewable potentials is adapted from the input parameters of energy system models developed at IIP [13] and based on the following factors:

- Topology and land cover based on [14] and [15],
- Existing infrastructure (electricity, gas and oil grid as well as rail and road infrastructure and seaways) derived from [16],
- Climatic conditions (solar irradiation, wind speed) according to [17],
- Protected areas according to [18] and
- Assumptions on cost degression for capital and operational costs based on the TYNDP 2022, scenario "Distributed Energy" [19].

Local costs of iron supply

From the above-mentioned site-specific electricity costs (levelized costs of electricity, LCOE), iron costs are derived by adding costs for electrolysis, hydrogen storage and iron reduction, which are assumed to be the same at each reduction site. Hydrogen is needed for thermo-chemical reduction of iron oxides as depicted in Figure 1.
The costs of hydrogen supply (levelized costs of hydrogen, LCOH) for the potential iron reduction sites are calculated in Equation (1). The first term covers capital ($CAPEX$), energy and O&M ($OPEX$) costs for proton exchange membrane (PEM) electrolyzers. PEM electrolyzers enable extremely flexible operation along local renewable electricity generation, eliminating the need for intermediary battery storage [20].
FLH_{RES} is the full load hours per year from local renewable energy sources and depends on where in Patagonia or the MENA region the electrolyzer is located, compare previous part. The produced hydrogen is fed into high-pressure storage tanks that decouple the operation of the electrolyzer and the iron reduction plant. Their investment and operational costs form the second term of the LCOH. The electricity used to store and release hydrogen into the pressurized storage is the third term. The hydrogen storage is sized to hold a three days' hydrogen production by the electrolyzer. η describes the efficiency of respective processes.
Annuity factors (ANF) of 0.087 and 0.073 are derived from depreciation periods of 20 and 30 years for the electrolyzer, hydrogen storage and reduction plant, respectively, and a 6 % interest rate. Parameter values for the electrolysis, hydrogen storage and iron reduction processes are listed in Table 1.

$$LCOH[€/MWh_{H2}] = \left[\frac{CAPEX_{Elec} \cdot (OPEX_{Elec} + ANF_{Elec})}{FLH_{RES}} + LCOE\right] \cdot \frac{1}{\eta_{Elec}} + \frac{3}{365} \cdot CAPEX_{Stor} \cdot (OPEX_{Stor} + ANF_{Stor}) + (1 - \eta_{Stor}) \cdot LCOE \quad (1)$$

As it is currently the most researched and advanced option for the decarbonization of the steel industry, the direct reduction of iron oxides with hydrogen takes place in a shaft furnace plant. The levelized costs of the product, fine iron powder (LCOI), include capital, energy (electricity and hydrogen) and O&M costs of the plant as in (2). The heating value of iron can be found in Table 7 in the Appendix.

$$LCOI[€/t_{Fe}] = \frac{1}{LHV_{Fe}} \cdot \Big[CAPEX_{Red} \cdot (OPEX_{Red} + ANF_{Red}) + h2_{Red} \cdot LCOH + el_{Red} \cdot LCOE \Big] \tag{2}$$

Table 1: Parameters for electrolysis, hydrogen storage and iron reduction process

	Value	**Unit**	**Reference Year**	**Reference**
Electrolyzer				
CAPEX_{Elec}	500 000	€/MW_{el}	2030	[21]
OPEX_{Elec}-Factor	5	%/a	2030	[21]
Efficiency η_{Elec}	67	%	2030	[21]
Lifetime	20	a	2030	[21]
ANF_{Elec}	0.087	a^{-1}		
200 bar hydrogen storage tank incl. compressor				
CAPEX_{Stor}	45 000	€/MWh_{H2}	2030	[22]
OPEX_{Stor}-Factor	1.11	%	2030	[22]
Electricity Consumption	4	$\text{MWh}_{el}/\text{t}_{H2}$	2030	[22]
Efficiency η_{Stor}	88	%	2030	[22]
Lifetime	30	a	2030	[22]
ANF_{Stor}	0.073	a^{-1}		
Iron reduction plant (shaft furnace)				
CAPEX_{Red}	230	€/(t_{Fe}/a)	2030	[23]
OPEX_{Red}-Factor	3	%	2030	[23]
Hydrogen Consumption h2_{Red}	635	$\text{Nm}^3/\text{t}_{Fe}$	-	[24]
	1.9	$\text{MWh}_{H2}/\text{t}_{Fe}$		
Electricity Consumption el_{Red}	0.31	$\text{MWh}_{el}/\text{t}_{Fe}$	-	[24]
Lifetime	20	a	2030	[23]
ANF_{Red}	0.087	a^{-1}		

3.2 Transport

Structure

Within the 50 km radius from the sea ports, where all considered electricity generation facilities are situated, the exact locations of hydrogen production and iron reduction plants are not fixed to ensure respecting local circumstances and enable aggregation of certain infrastructures. Consequently, since the commodity (electricity, hydrogen or iron) is not defined within the first

two levels, i.e., from the wind or solar farms to the sea ports and vice versa, cf. Figure 2, transportation (and associated costs and emissions) is neglected until the sea port is reached. As only transport after the seaport of the exporting country is considered, the only transported commodity throughout the network is iron (in Mt). For route distances, we utilize the EcoTransIT World Emission calculator [25] or the searoute distance tool [26].
It is assumed that each port has the structure and sufficient capacity to process the amount of iron or iron oxide, neglecting investment costs. During transport between consecutive levels, cf. Figure 2, dynamic switching of transportation modes is not possible. Instead, we give different static transportation options like barge, train or sea vessel from which the optimization can choose.
As intermediate hubs for landing the oversea freight and starting inland distribution, we consider the ports of Rotterdam and Wilhelmshaven, while other German sea ports are only used for the supply of adjacent power plants. The choice of Rotterdam and Wilhelmshaven is justified in the fact that they handle most of European/German imports for hard coal in Europe [27] and Germany [28], respectively.
In Germany, we assume that due to the similarity in handling as dry bulk, the transporting infrastructure for hard coal can be re-used for iron. Thus, we neglect investment costs for inland transport (barges, trains, ports, train stations). In contrast to lignite, hard coal is an import good for Germany and therefore the infrastructure for handling and transporting hard coal exists and power plants are situated either along rail tracks, at sea ports or along inland waterways. We respect the local circumstances by only allowing locally available transport modes, see Table 8.

Costs

We divide the costs for transport into variable costs and fixed costs and further into transport costs over edges and costs at nodes. As mentioned before, all costs are inflation-adjusted to the year of 2030.
We approximate the variable transport costs via the average energy consumed per Mt of transported good and kilometers and the corresponding fuel or energy costs of the specific mode of transport. Maintenance and service costs are added when available whereas capital costs are disregarded as we assume the re-utilization of coal infrastructure. For routes passing the Suez, Panama or Kiel canal, we calculate the total canal cost by approximating the amount of passing vessels linearly.
For sea vessels we assume an average speed of 24.08 km/h or 13 kn [29, 30] and the use of VLSFO (Very Low Sulphur Oil) as fuel (80% MGO: Marine Gas Oil and 20 % HFO: Heavy Fuel Oil). We use an average fuel cost of 49.13 €/MWh [31] and an average consumption of 57.35 t/d [30, Table 54] (derived via heating values from Marine Diesel Oil). Together with the (lower) heating value of VLSFO, 11.72 TWh/Mt [31, Sec. 4.6.2], we receive consumption costs of 1 380 €/h. Furthermore, we assume operational costs of 440 €/h [30, Table 54]. Supposing an average capesize vessel capacity of 155 000 dwt (dead weight tonnage) [29] leads to an overall cargo rate of 0.049 ct/(t·km).
For distances, we use data obtained from [26] and receive travel cost of 1.51 € to 17.65 € per transported ton depending on the route. This cargo rate is sligthly outsides the range reported in [30] (0.06–0.9 ct/(t·km), but as we disregard capital costs which are 40 % of the published costs and the date of the publication (2010) this can be expected.
Additionally, we consider canal costs of 475 000 € per vessel at the Suez Canal [32, 33], 395 000 € per vessel for the Panama Canal [34] and 6 900 € per vessel for the Kiel Canal [35]. The Suez Canal gets passed for imports from United Arab Emirates, Qatar, Saudi Arabia, Jordan,

Kuwait, Iraq and partly Israel, the Panama Canal only for some imports from Chile and the Kiel Canal only if Rostock is provided with iron by sea vessel. Alternative routes via Cape Horn or Cape of Good Hope are not considered. We disregard limitations for vessel size for the Panama and Kiel Canal since we approximate cost linearly. For passing the Suez Canal there are no relevant limitations since after its expansion in 2015 almost every cape-sized bulk carriers can pass it [36].
For each port, fixed costs of 70 000 € per ship are applied. Here, we use the port fees of Rotterdam [37] as estimate for all port fees. For the power plants located in Wilhelmshaven, Hamburg and Rostock, we assume that they can be supplied directly with bulk carriers from sea.
For barges we assume the usage of diesel-fueled 2×2 push convoys with 11 200 t of capacity [38] and take a distance-weighted average of the cost per ton from Rotterdam to Höchst and Rotterdam to Karlsruhe from [39] to receive a general cargo rate for barges of 2.04 ct/(t·km). For trains, we assume 1700 t of capacity and an average speed of 100 km/h based on the data provided by [38] and a cargo rate of 2.86 ct/(t·km) [40]. Since 92 % of the German rail freight transport is electric [41], we assume that all trains are powered by the electrical grid. As variable processing cost per node we assume 4.23 €/t for sea ports [37] and 3.91 €/t for river ports as loading cost [39].
An overview of the transport costs applied in the case study is displayed in Table 2.

Efficiency

For each transport section, the lost energy is calculated in relation to the transported or produced energy. Conceptually, it is easy to extend the calculations with further consumers of energy for more detailed efficiency calculations. We calculate the efficiencies in the network by using a flow-weighted average over the efficiencies of the respective processes. We do not consider energy consumed during loading and unloading of cargo due to missing data.
By building the ratio between transport energy demands (cf. assumptions in Table 2 and 7) and the transported energy inherent in the iron, we can calculate the efficiency of the respective route and transport mode, $\frac{E_{Fe}-E_{trans}}{E_{Fe}}$.
For calculating the overall transport efficiency, we average the individual efficiencies weighted with their flow over the overall forward flow through the network. We obtain the overall forward flow by summing all flows between two levels. By averaging over the overall flow in forward direction, we indirectly respect the increase in consumed energy through the heavier cargo/greater flow when returning the iron oxide.
The individual calculations for the transport modes can be examined in the Table 3. Necessary data can be found in Table 7 and 2.

Table 2: Parameters for Transport Costs

	Value	Unit	Reference Year	Reference
Dry Bulk Carrier				
Dead Weight Tonnage	155 000	dwt	-	[29]
Gross Tonnage	82 500	Gt	-	[42]
Average Speed	24.08	km/h	-	[29]
Fuel Consumption	57.35	t_{VLSFO}/d	2010	[31, 30]
Fuel Cost	1 380	€/h	2030	[31]
Operational Costs	440	€/h	2010	[30, Table 54]
Cargo Rate	0.049	ct/(t·km)	-	-
Barge				
Dead Weight Tonnage	11 200	t	-	[38]
Average Speed	10.05	km/h	-	[38]
Cargo Rate	2.04	ct/(t·km)	2000	[39, Tab. 2]
Train				
Dead Weight Tonnage	1 700	t	-	[38]
Average Speed	100	km/h	-	[43]
Cargo Rate	2.86	ct/t·km	2019	[40]
Costs at Ports				
Port Fees	70 000	€ per Ship	2021	[37]
Seaside Processing Costs	4.23	€/t	2021	[37]
Inland Processing Costs	3.91	€/t	2006	[39, Fig. 6]
Canal Fees				
Suez Canal	475 000	€ per Ship	2022	[32, 33]
Panama Canal	395 000	€ per Ship	2023	[34]
Kiel Canal	6 900	€ per Ship	2022	[35]

Table 3: Transport Efficiencies of different Transportation Modes

Transport Mode	**Efficiencies**
Carrier η_{uv}:	$1 - \frac{H_{VLSFO} \cdot 55 \frac{t}{h} \cdot \Delta d \cdot v}{24 \cdot H_{Fe} \cdot m_{carrier}}$
Barge η_{uv}:	$1 - \frac{P_{engine} \cdot \Delta d \cdot v}{\eta_{engine} \cdot H_{Fe} \cdot m_{Barge}}$
Train η_{uv}:	$1 - \frac{E_{cons}[kWh/t \cdot km] \cdot \Delta d \cdot m_{train}}{H_{Fe} \cdot m_{train}}$
Total Transport Efficiency η:	$1 - \frac{\sum_{(u,v) \in E} (1-\eta_{uv}) Q_{u,v}}{\sum_{(i,j) \in L_1 \times L_2} Q_{ij}}$

CO_2-Emissions

Similar to the calculation of efficiencies and fuel costs, we derive a third key figure, the CO_2-emissions of transportation, through an approximation of fuel or energy consumption. Analogously to the costs, emissions of the construction or retrofit of facilities and infrastructure are not considered.
For trains, we use the average CO_2-equivalent emissions per kilowatt hour of German electricity generation in the year 2020, 313 g_{CO_2}/kWh_{el} [44] to estimate an emission factor in electricity generation of 100 g/kWh for the year 2030 based on the goals of the federal German government for an 80 % share of RES in electricity generation [45]. Fuel-based emissions for barges operated with diesel are assumed to be 3.165 t_{CO_2}/t_{Diesel} [46] and for carriers operated with VLSFO 3.188 t_{CO_2}/t_{VLSFO} [31, Sec. 4.6.1]. The equations for calculating CO_2-emissions are displayed in Table 4. Necessary data can be found in Table 7.

Table 4: Transport Emissions of different Transportation Modes

Transport Mode	**t CO_2-Emissions per transported Mt**
Carrier:	$\frac{55 \frac{t}{h} \cdot \Delta d \cdot v}{24 \cdot m_{vessel}} \cdot 3.188 \ \frac{t_{CO_2}}{t}$
Barge:	$\frac{P_{engine} \cdot \Delta t}{\eta_{engine} \cdot H_{diesel} \cdot m_{train}} \cdot 3.165 \ \frac{t_{CO_2}}{t}$
Train:	$\frac{E_{cons}[kWh/(t \cdot km)] \cdot \Delta d \cdot m_{train}}{m_{train}} \cdot 100 \ \frac{g_{CO_2}}{\text{kWh}}$

3.3 Importing Country

Iron demand

A fixed demand for iron serves as the optimization's driving factor. We presume that all hard coal-fired power plants that are still in operation in 2030 will have undergone full conversion to iron. Owing to the fact that lignite-fired power plants are located close to the extraction area and lack the necessary transportation infrastructure for the import of coal from overseas, we only consider the retrofit of hard coal-fired power plants that have this infrastructure (ports or railroad connection), which we assume could be fully re-used for iron transport.
In a rather conservative scenario, the German federal network agency (Bundesnetzagentur) lists 39 hard coal-fired power plants with a total electricity generation capacity of 13.5 GW in operation in 2030 [47]. Assuming that the conversion to iron is only worthwhile for power plants with capacities greater than 100 MW, 25 power plants with a total electricity generation capacity of just under 13 GW remain.
We assume a consistent utilization of 50 % or 4 380 hours annually. This is a rather conservative assumption because as the resulting energy would be regarded as renewable energy, utilization could potentially be higher. All 25 power plants together will then require approximately 59 million tons of iron per year to produce 56 TWh of electricity using iron powder with a heating value of 2.05 MWh per ton and a consistent total power plant efficiency of 46.4 % [4], assuming that 100 % of iron is transformed into iron oxide. Name, location, (inland) port, railway connection and annual iron demand for the 25 power plants included in the optimization are shown in Table 8 in the Appendix.

Costs at Iron Power Plants

Assuming no capital expenditures because the expenses of the retrofit from coal to iron are unknown at the moment while first studies indicate that they are minor [4], solely operational costs at the power plants are taken into account. Owing to the lack of data on iron power plants resulting from the fact that no industrial scale iron power plants are in operation yet, fixed and variable operational costs of hard-coal power plants are used: 29.37 euros per installed kW electricity generation capacity per year, divided by an annual utilization of 4 380 hours, and 0.53 cents per kWh generated electricity [48]. Both are current values which were inflation-adjusted to use them for the target year 2030.

4 Results

In the following we present the results of the case study based on the method and parameters described in the previous sections. Further, we will contextualize costs to electricity generation from coal, estimating a break-even CO_2 price at which iron could be competitive.

4.1 Case Study

Figure 3 shows the selected sites in the results together with their transport routes. As regions for iron reduction, we receive coastal areas in Western Sahara providing 44.88 % of the iron for export, at the Strait of Magellan in Chile with 37.90 %, in southern Argentina with 16.81 % and lastly in Morocco providing 0.41 % from Essaouira.

The shares for Western Sahara are further divided into 23.99 % in Laâyoune and 20.89 % in Dakhla. In Chile 37.32 % origins from Caleta Clarencia at the Bay Gente Grande and 0.58 % from the Terminal Cabo Negro, north of Punta Arenas. The imports from Argentina are provided from 13.22 % from San Sebastián, 3.07 % from Puerto Deseado and 0.52 % from Río Gallegos.

The selection of regions in Patagonia may seem surprising due to the distance of approximately 14 000 kilometers to Rotterdam/Wilhelmshaven. Our findings support the statement of Berenschot [49], that the mayor cost driver for iron fuels are electricity costs, as the selected energy export regions coincide with cost-minimal RES potentials in the input data. The overall average for LCOE over all input data is 20.07 €/MWh. The selected sites have an average of 8.95 €/MWh with some wind parks in Argentina and Chile even having LCOE of less than 8 €/MWh.

Averaged over all reduction sites, the costs are composed as follows: 57.31 % from the iron reduction, 21.03 % from processing cargo at Ports/Hubs, 13.00 % from transport costs, 8.66 % from costs for the oxidation, 0.01 % from port fees and 0.003 % from canal cost.

Overall, we fulfill 91.42 % of the demand with onshore wind parks. The rest is one 4 316 MW offshore wind park off the coast of Dahkla. Electricity generation from concentrating solar power plants or photovoltaic facilities are not part of the solution.

Arriving in Europe, 23.63 % of the iron imports are directly supplied to power plants with sea ports. The rest is transshipped over Rotterdam (72.70 %) and Wilhelmshaven (3.67 %). As inland transport by barge is cheaper than by train, iron for the inland power plants is provided in 92.53 % of the cases by barge and only in 7.47 % by train. Those plants supplied by train are plants which can not be supplied via inland or seaside ports due to the lack of a port.

We obtain average electricity generation costs of 13.91 ct/kWh_{el} for iron-based electricity generation with former German hard-coal power plants. We have to keep in mind that these

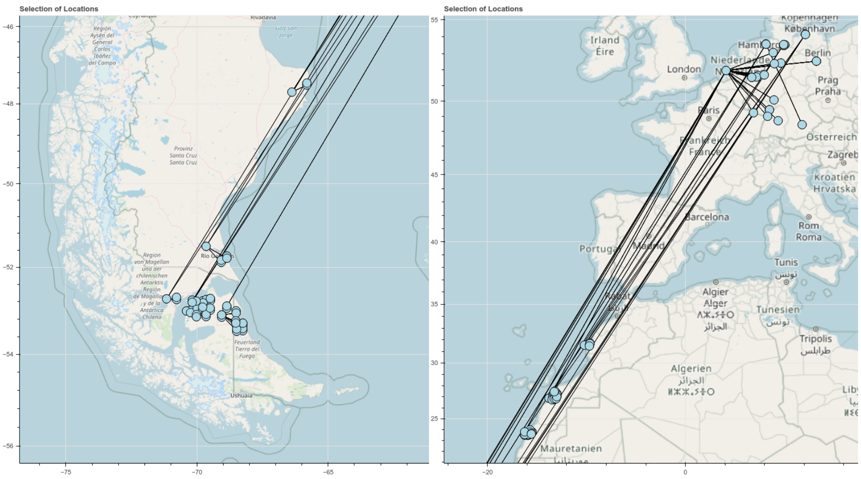

Figure 3: Logistic Network for supplying Germany with iron in 2030

costs are not electricity generation costs in the conventional sense, since we neglect investment or retrofit costs for power plants and transportation infrastructure, assuming the (re-)use of existing infrastructure.

The overall efficiency of the closed iron cycle, averaged over all considered power plant sites and energy export regions, is 27.47 %. This efficiency originates from fixed efficiencies of 60 % for the reduction process [8] and 46.4 % as total efficiency of the oxidation plant [4] as well as an average transport efficiency, dependent on the respective transport distance and mode of transport, of 98.68 %, see Section 3.2. As average emissions we get 60.77 g_{CO_2}/kWh_{el}.

The characteristic numbers of this case study, averaged over all considered power plant sites, can be found in Table 5.

Table 5: Key Values of the Case Study

Parameter	**Value**	**Unit**
Total Costs	7 834 999 857	€
Total RES Electricity Generation	56.34	TWh
Total Iron Demand	59.23	Mt_{Fe}
Total CO_2-Emissions	3 423 974	t_{CO_2}
Average Electricity Generation Costs from Iron	13.91	ct/kWh_{el}
Average Emissions per kWh_{el}	60.77	g_{CO_2}/kWh_{el}
Average Cycle Efficiency	27.47	%

4.2 Influence of CO_2-Pricing

If CO_2-prices are taken into account for transportation by means of their CO_2-emission factor as described in Section 3.2 and displayed in Table 4, we see changes in the selection of sites. The changes for different hypothetical CO_2-prices are displayed in Table 6. The further we increase the CO_2-price, the more the optimization selects locations closer to Germany while at the same time the share of imports from remote sites in Patagonia decreases. For example, by increasing the CO_2-price to a hypothetical value of 260 € per ton of emitted CO_2, no sites in South America are selected anymore. With an increase in CO_2-price, the overall cost for one kilowatt hour electricity increases as well, while emissions decline. The increase in efficiency is neglectable (less than 0.2 %).

Table 6: Influence of key values

CO_2-Price [€/t_{CO_2}]	**Selection**	**Costs** [ct/kWh_{el}]	**Emissions** [g_{CO_2}/kWh_{el}]
0	See Fig. 3	13.91	60.77
20	~~Terminal Cabo Negro (CHL)~~	14.03	59.88
50	~~Río Gallegos (ARG)~~, ~~Puerto Deseado (ARG)~~	14.20	57.40
60	Tunis (TUN)	14.26	53.08
130	Adschabiya (LBY)	14.61	48.03
170	Tobnuk (LBY)	14.79	43.81
200	~~CHL~~	14.91	39.93
240	Safaga (EGY)	15.07	37.48
260	~~ARG~~	15.14	34.36
280	~~EGY~~	15.21	34.33

4.3 Comparison to Coal-based Electricity Generation

Finally, electricity generation costs are contextualized by comparing them to hard coal electricity generation. The CO_2-price at which running a fictitious power plant on iron would be less expensive than running it on coal is estimated in a rough calculation.
To ensure comparability, coal and iron are assumed to arrive at the power plant via the same route with logistics costs of 45.02 €/t for iron. Supposing the use of the same infrastructure and thus the same transport costs per cubic meter, logistics costs for coal are higher with 49.88 €/t due to the much lower density of 1 300 kg/m^3 compared to 3 500 kg/m^3 for iron powder. Likewise, using a mass factor of 1+1.43 between oxidized and reduced iron powder, 57.81 kg_{CO_2}/t emissions along the transport chain for iron (outbound and return journey) result in 64.05 kg_{CO_2}/t for coal (only one way). For product supply in the exporting region, we assume coal costs of 75 €/t [48] versus LCOI of 75.80 €/t (range: 70.94 - 88.60 €/t), resulting from electricity costs with a weighted average of 9.43 €/MWh at the selected locations.
In the import region, power plant full load hours and operational costs are set equal to those used for iron power plants (4 380 hours per year; 29.37 €/kW per year and 0.53 ct/kWh [48], see 3.3). The efficiency of the coal power plant is assumed to be 46 % [48] compared to 46.4 % for the iron power plant [4]. Carbon dioxide emissions from coal combustion in the power plant are considered with an emission factor of 337 g_{CO_2}/kWh_{Coal} [50]. We use a heating value of 8.06 kWh/kg for hard coal (see Table 7).
Costs for electricity generation can be expressed as a function of CO_2-price as in Equation (3) for coal-based and in Equation (4) for iron-based electricity generation. As investment costs of the power plant and transportation infrastructure are not considered, since the use of existing infrastructure is implied, those costs cannot be understood as electricity generation costs in

the conventional sense. Nonetheless, they can be used to estimate the break-even CO_2-price of iron and coal-based electricity generation. Our calculation of coal electricity generation costs (4.57 ct/kWh_{el} without CAPEX and CO_2-pricing) is in accordance with recent literature [48].

$$
\begin{aligned}
C_{Coal} =& \frac{75 \frac{€}{t_{Coal}} + 49.88 \ \frac{€}{t_{Coal}}}{0.46 \frac{kWh_{el}}{kWh_{th}} \cdot 8.06 \ \frac{kWh_{th}}{kg_{Coal}}} + \frac{29.37 \frac{€}{kW_{el}}}{4\,380 \ h} + 0.53 \frac{ct}{kWh_{el}} + \frac{337 \frac{g_{\mathrm{CO_2}}}{kWh_{th}} + \frac{64.05 \frac{kg_{\mathrm{CO_2}}}{t_{Coal}}}{8.06 \ \frac{kWh_{th}}{kg_{Coal}}}}{0.46 \frac{kWh_{el}}{kWh_{th}}} \cdot P_{\mathrm{CO_2}} \\
=& 4.57 \frac{ct}{kWh_{el}} + 750 \ \frac{g_{\mathrm{CO_2}}}{kWh_{el}} \cdot P_{\mathrm{CO_2}} \qquad (3) \\
C_{Fe} =& \frac{75.80 \frac{€}{t_{Iron}} + 45.02 \ \frac{€}{t_{Iron}}}{0.464 \frac{kWh_{el}}{kWh_{th}} \cdot 2.05 \ \frac{kWh_{th}}{kg_{Iron}}} + \frac{29.37 \frac{€}{kW_{el}}}{4\,380 \ h} + 0.53 \frac{ct}{kWh_{el}} + \frac{57.81 \frac{kg_{\mathrm{CO_2}}}{t_{Iron}}}{2.05 \ \frac{kWh_{th}}{kg_{Iron}} \cdot 0.464 \frac{kWh_{el}}{kWh_{th}}} \cdot P_{\mathrm{CO_2}} \\
=& 13.91 \frac{ct}{kWh_{el}} + 60.77 \ \frac{g_{\mathrm{CO_2}}}{kWh_{el}} \cdot P_{\mathrm{CO_2}} \qquad (4)
\end{aligned}
$$

By equating (3) and (4), a break-even CO_2-price of $P_{CO_2} = 135.5$ €/$t_{\mathrm{CO_2}}$ is obtained. According to this rough calculation, using iron instead of coal would be economical when CO_2-prices exceed 135.5 €/$t_{\mathrm{CO_2}}$, under neglection of uncertain retrofit costs for power plants and transportation infrastructure.

One could argue that another network configuration with shorter distances would give us a lower break-even point since shorter distances lead to less emissions, therefore influencing the calculation of the break-even point. But the opposite is the case. If we use the network design obtained with a CO_2-price of 280 €/$t_{\mathrm{CO_2}}$, c.f. last row of Table 6, we get an even higher break-even point of 140 €/t, because the lower costs in logistics are getting compensated by higher LCOI.

The operation of coal-fired power plants is subject to the regulations of the European Emissions Trading System (EU-ETS), which will soon include international shipping. As of April 2023, the current all-time high for the price of emission allowances is around 105 €/$t_{\mathrm{CO_2}}$ and occurred in February 2023. Our estimated break-even-price of 135.5 €/$t_{\mathrm{CO_2}}$ is not too far from current prices.

5 Model Discussion and Outlook

We presented a first network-based site selection and transport optimization model for the use of iron as an energy carrier. The model was used for conducting a case study where all German hard coal power plants expected to potentially still operate in the year 2030 are operated with iron. The estimated renewable energy potentials of coastal regions in 16 countries in the MENA region and Patagonia set the base for an identification of cost-minimal iron reduction sites. A method for calculating iron supply costs from local electricity costs and costs for electrolysis and iron reduction was presented. We gained first indications on the costs and CO_2-emissions associated with electricity generation from iron as well as for energy partnerships for an iron-based circular energy economy. In our case study, producing one megawatt hour of electricity from iron results in costs of 139.1 Euros on average in 2030. For the reduction process, locations in Western Sahara, Chile, Argentina and Morocco are chosen within the optimization.

5.1 Critical Review and Model Extension

Concerning electricity generation costs, it is important to point out that retrofit or construction costs for power plants and transport infrastructure are not included since no reliable cost estimates exist yet. Emissions associated with the retrofit or construction of infrastructure are also not included. Also, we neglect costs and emissions associated with the transport of hydrogen or electricity within the 50 kilometers radius around the seaports in the exporting regions as well as energy consumed for cargo handling at the network nodes.

The results of the case study must be seen in the light of high uncertainties. The major limitation of the proposed optimization problem lies in the lack of reliable data with global coverage, for example regarding costs and efficiencies of iron reduction and oxidation processes or the future availability of coal infrastructure. Increasing the validity of the model results through sensitivity analysis and parameter studies regarding those aspects is in the scope of our ongoing research.

Since variable costs associated with conversion and processing are fully linear, economies of scale are not incorporated. In reality, however, it is likely that aggregation will evolve along the entire supply chain. Scale effects should thus be implemented when further developing the model.

Furthermore, the model could be rewritten as a time-dependent problem to include aspects such as shortages or non-availabilities and storage requirements. The logistic network could be enhanced by adding more transshipment ports, port capacities (currently, iron for inland power plants is transferred via either Rotterdam or Wilhelmshaven without any limitations at ports) and the ability to dynamically switch between means of transport on the route, especially between seaports and power plants.

Another possibility for future development is to include more regions as potential reduction sites, until worldwide coverage is achieved. In addition to local renewable energy potentials and electricity generation costs, there may be further distinction in the evaluation of regions worldwide regarding their suitability for the reduction process, for example by including country-specific WACC, investment, labor and operational costs.

Regarding the selection of reduction sites in the light of country risks, the optimizations' choice of areas in Western Sahara is questionable, as external sources report political instability. Thus, including socio-political aspects is desirable and could be accomplished by incorporating country rankings regarding criteria such as political stability or corruption. Furthermore, in order to improve the robustness of the optimization, the risk of infrastructure outages along the supply chain or among the export countries should be addressed. The implementation of both aspects into a network optimization are subject of our current research in the *Clean Circles* project.

5.2 Conclusions and Outlook

A site selection and logistic optimization model was developed and tested using a simplified case study. In addition to the presentation of the model's general adequacy, predictions on costs, emissions and efficiencies related to electricity generation from iron as well as a first estimate on the order of magnitude of a CO_2-price at which iron-based electricity generation is economical compared to coal was made. The estimated break-even CO_2-price of 135.5 €/t_{CO_2} encourages further research into the use of iron as an energy carrier.

The next phase will include further development of the site selection and logistic optimization model as described in the previous section. The ultimate objective is to include other energy carriers to directly compare the use of iron to other options such as hydrogen, methanol, ammonia, liquid organic hydrogen carriers, and so on, in a model-based approach. It will be investigated how energy carriers can be used in a future energy system in a complementary manner and what role reactive metals, specifically iron, might play. The focus will be expanded to include other sectors, such as industry, commerce and services, heat and transport in addition to electricity generation. This is a key element of the *Clean Circles* cluster initiative.

References

[1] Energiewirtschaftliches Institut an der Universität zu Köln (EWI). *dena-Leitstudie Aufbruch Klimaneutralität. Klimaneutralität 2045 - Transformation der Verbrauchssektoren und des Energiesystems.* Herausgegeben von der Deutschen Energie-Agentur GmbH (dena). Oct. 2021. URL: https://www.ewi.uni-koeln.de/cms/wp-content/uploads/2022/03/211005_EWI-Gutachterbericht_dena-Leitstudie-Aufbruch-Klimaneutralitaet.pdf.

[2] Jeffrey M. Bergthorson. *Recyclable metal fuels for clean and compact zero-carbon power.* In: Progress in Energy and Combustion Science 68 (2018), pp. 169–196. ISSN: 0360-1285. DOI: https://doi.org/10.1016/j.pecs.2018.05.001.

[3] Luc Dirven, Niels G. Deen, and Michael Golombok. *Dense energy carrier assessment of four combustible metal powders.* In: Sustainable Energy Technologies and Assessments 30 (2018), pp. 52–58. ISSN: 2213-1388. DOI: https://doi.org/10.1016/j.seta.2018.09.003.

[4] Johannes Janicka et al. *The potential of retrofitting existing coal power plants: a case study for operation with green iron.* 2023. arXiv: 2303.04000 [eess.SY]. URL: https://arxiv.org/abs/2303.04000.

[5] Technische Universität Darmstadt. *Clean Circles Cluster Project.* 2023. URL: https://www.tu-darmstadt.de/clean-circles/about_cc/index.en.jsp (visited on 03/27/2023).

[6] Tao Li et al. *Visualizing particle melting and nanoparticle formation during single iron particle oxidation with multi-parameter optical diagnostics.* In: Combustion and Flame 245 (2022). ISSN: 0010-2180. DOI: https://doi.org/10.1016/j.combustflame.2022.112357.

[7] Paulo Debiagia et al. *Iron as a sustainable chemical carrier of renewable energy: Analysis of opportunities and challenges for retrofitting coal-fired power plants.* In: Renewable and Sustainable Energy Reviews 165 (2022). ISSN: 1364-0321. DOI: https://doi.org/10.1016/j.rser.2022.112579.

[8] Jannik Neumann et al. *Techno-economic assessment of long-distance supply chains of energy carriers: Comparing hydrogen and iron for carbon-free electricity generation.* 2023. arXiv: 2303.00681 [physics.soc-ph].

[9] Ksenia Bestuzheva et al. *The SCIP Optimization Suite 8.0.* Technical Report. Optimization Online, Dec. 2021. URL: http://www.optimization-online.org/DB_HTML/2021/12/8728.html.

[10] European Central Bank. *HICP - Overall Index.* URL: https://sdw.ecb.europa.eu/quickview.do?SERIES_KEY=122.ICP.A.D0.N.000000.4.AVR (visited on 04/22/2023).

[11] European Central Bank. *ECB staff macroeconomic projections for the euro area.* URL: https://www.ecb.europa.eu/pub/pdf/other/ecb.projections202303_ecbstaff~77c0227058.en.pdf.

[12] European Central Bank. *Two percent inflation target.* URL: https://www.ecb.europa.eu/mopo/strategy/pricestab/html/index.en.html.

[13] Viktor Slednev et al. *Highly resolved optimal renewable allocation planning in power systems under consideration of dynamic grid topology.* In: Computers Operations Research 96 (2018), pp. 281–293. ISSN: 0305-0548. DOI: https://doi.org/10.1016/j.cor.2017.12.008. URL: https://www.sciencedirect.com/science/article/pii/S0305054817303088.

[14] National Centers for Environmental Information. *Global Relief Model. Version ETOPO1.* 2009. DOI: 10.7289/V5C8276M. URL: https://www.ncei.noaa.gov/products/etopo-global-relief-model.

[15] Marcel Buchhorn et al. *Copernicus Global Land Service: Land Cover 100m: collection 3: epoch 2019: Globe*. Version V3.0.1. Sept. 2020. DOI: 10.5281/zenodo.3939050.

[16] OpenStreetMap contributors. *Map Data*. URL: https://download.geofabrik.de/.

[17] Copernicus Climate Change Service (C3S). *ERA5: Fifth generation of ECMWF atmospheric reanalyses of the global climate*. 2017. URL: www.ecmwf.int/en/forecasts/datasets/reanalysis-datasets/era5.

[18] UNEP-WCMC and IUCN. *Protected Planet: The World Database on Protected Areas (WDPA) and World Database on Other Effective Area-based Conservation Measures (WD-OECM).* Cambridge, UK. 2021. URL: www.protectedplanet.net.

[19] ENTSO-E and ENTSO-G. *TYNDP 2022 Scenario Report – Version April 2022*. 2022. URL: https://2022.entsos-tyndp-scenarios.eu/download/.

[20] Sarah Milanzi et al. *Technischer Stand und Flexibilität des Power-to-Gas-Verfahrens*. Working Paper Energie und Ressourcen, TU Berlin. Aug. 2018. DOI: 10.5281/zenodo.2620254.

[21] Markus Hurskainen. *Liquid organic hydrogen carriers (LOHC): Concept evaluation and techno-economics*. VTT Research Report No. VTT-R-00057-19. VTT Technical Research Centre of Finland, Dec. 2019. URL: https://cris.vtt.fi/en/publications/liquid-organic-hydrogen-carriers-lohc-concept-evaluation-and-tech.

[22] Johannes Hampp, Michael Düren, and Tom Brown. *Import options for chemical energy carriers from renewable sources to Germany.* In: PLoS ONE 18(2) (Feb. 2023). DOI: https://doi.org/10.1371/journal.pone.0281380.

[23] Valentin Vogl, Max Åhman, and Lars J. Nilsson. *Assessment of hydrogen direct reduction for fossil-free steelmaking.* In: journaltitle of Cleaner Production Volume 203 (Dec. 2018), pp. 736–745. ISSN: 0959-6526. DOI: https://doi.org/10.1016/j.jclepro.2018.08.279.

[24] Marc Hölling, Matthias Weng, and Sebastian Gellert. *Bewertung der Herstellung von Eisenschwamm unter Verwendung von Wasserstoff.* 2017. URL: https://germany.arcelormittal.com/icc/arcelor/med/b8e/b8e0c15a-102c-d51d-b2a9-147d7b2f25d3,11111111-1111-1111-1111-111111111111.pdf.

[25] IVE GmbH ifeu INFRAS und Fraunhofer IM. *EcoTransIT World Emissionsrechner*. URL: https://www.ecotransit.org/de/emissionsrechner/.

[26] Gent Halili. *Seaorute Python Package*. URL: https://github.com/genthalili/searoute-py.

[27] Global Energy Monitor Wiki. *Port of Rotterdam*. URL: https://www.gem.wiki/Port_of_Rotterdam (visited on 04/04/2023).

[28] Global Energy Monitor Wiki. *Port of Wilhelmshaven*. URL: https://www.gem.wiki/Port_of_Wilhelmshaven (visited on 04/04/2023).

[29] Dariusz Bernacki. *Assessing the Link between Vessel Size and Maritime Supply Chain Sustainable Performance*. In: Energies 14.11 (2021). ISSN: 1996-1073. DOI: 10.3390/en14112979. URL: https://www.mdpi.com/1996-1073/14/11/2979.

[30] Eef Delhaye et al. *COMPASS The COMPetitiveness of EuropeAn Short-sea freight Shipping compared with road and rail transport*. Transport Mobility Leuven. URL: https://www.schonescheepvaart.nl/downloads/rapporten/doc_1361789985.pdf (visited on 03/24/2023).

[31] Anouk van Grinsven, Dagmar Nelissen, Emiel van den Toorn, Jasper Faber, Reinier van der Veen. *Availability and costs of liquefied bio- and synthetic methane. The maritime shipping perspective*. URL: https://ce.nl/publicaties/availability-and-costs-of-liquefied-bio-and-synthetic-methane-the-maritime-shipping-perspective/.

[32] Suez Canal Authority. *Tolls Table 2022*. URL: https://www.suezcanal.gov.eg/English/Navigation/Tolls/Pages/TollsTable.aspx.

[33] Leth Agencies. *Suez Canal Toll Calculator*. URL: https://lethagencies.com/suez-calculator?Port=SUEZTREG&CTBreakdown=True&PortName=Suez+Canal+Transit&ETA=2023-04-22&CB2=03&TariffYear=22&SCNT=81578&GRT=82500&SCGRT=&Draft=&SDR=&Beam=&LadenBallast=true&NBorSB=true&GasFree=.

[34] Canal de Panamá. *Panama Canal Tolls*. URL: https://pancanal.com/wp-content/uploads/2021/08/1010-ingles.pdf.

[35] Bundesministerium der Justiz. *Verordnung über die Befahrungsabgaben auf dem Nord-Ostsee-Kanal (NOKBefAbgV)*. URL: https://www.gesetze-im-internet.de/nokbefabgv/BJNR518500993.html.

[36] Suez Canal Authorities. *Canal Characteristics*. URL: https://www.suezcanal.gov.eg/English/About/SuezCanal/Pages/CanalCharacteristics.aspx.

[37] Port of Rotterdam. *General Terms and Conditions including Port Tariffs*. 2021. URL: https://www.portofrotterdam.com/sites/default/files/2021-11/general-terms-and-conditions-including-port-tariffs-2021.pdf.

[38] EcoTransIT World Initiative. *Environmental Methodology and Data Update 2020*. URL: https://www.ecotransit.org/wordpress/wp-content/uploads/20210531_Methodology_Report_EcoTransIT_World.pdf.

[39] Prognos AG. *Variantenvergleich Küste versus Binnenland (2006)*. URL: https://docplayer.org/32866845-Variantenvergleich-kueste-versus-binnenland.html.

[40] Allianz pro Schiene e. V. *Externe Kosten*. URL: https://www.allianz-pro-schiene.de/glossar/externe-kosten/.

[41] Allianz pro Schiene e. V. *Güterverkehr - Mehr Verkehr auf die Schiene*. URL: https://www.allianz-pro-schiene.de/themen/gueterverkehr/.

[42] VesselFinder. *Vessels Database*. URL: https://www.vesselfinder.com/vessels?type=401&minDW=150000&maxDW=160000&dir=2&sort=4.

[43] Forschungsinformationssystem / Technische Universität Hamburg-Harburg Institut für Logistik und Unternehmensführung. *Betriebstechnische Grenzparameter für Güterzüge*. URL: www.forschungsinformationssystem.de/servlet/is/324625/.

[44] European Environment Agency. *Greenhouse gas emission intensity of electricity generation in Europe*. URL: https://www.eea.europa.eu/ims/greenhouse-gas-emission-intensity-of-1.

[45] Bundesregierung. *Koalitionsvertrag 2021-2025 zwischen der Sozialdemokratischen Partei Deutschlands (SPD), Bündnis 90/Die Grünen und den Freien Demokraten (FDP)*. URL: https://www.spd.de/fileadmin/Dokumente/Koalitionsvertrag/Koalitionsvertrag_2021-2025.pdf.

[46] Kristina Juhrich. *CO2-Emissionsfaktoren für fossile Brennstoffe*. Umweltbundesamt, 2016. URL: https://www.umweltbundesamt.de/sites/default/files/medien/1968/publikationen/co2-emissionsfaktoren_fur_fossile_brennstoffe_korrektur.pdf.

[47] Bundesnetzagentur. *Genehmigung des Szenariorahmens 2019-2030*. 2018. URL: https://www.netzentwicklungsplan.de/sites/default/files/paragraphs-files/Szenariorahmen_2019-2030_Genehmigung_0_0.pdf.

[48] Christoph Kost et al. *Stromgestehungskosten Erneuerbare Energien*. Fraunhofer-Institut für Solare Energiesysteme ISE, June 2021. URL: https://www.ise.fraunhofer.de/content/dam/ise/de/documents/publications/studies/DE2021_ISE_Studie_Stromgestehungskosten_Erneuerbare_Energien.pdf.

[49] Berenschot. *Techno-economic feasibility study of the Iron Fuel ecosystem*. URL: https://www.metalot.nl/pdf/Techno-economic%20feasibility%20study%20of%20the%20Iron%20Fuel%20ecosystem.pdf (visited on 03/06/2023).

[50] Kristina Juhrich. *CO2-Emissionsfaktoren für fossile Brennstoffe*. ISSN 1862-4359. Umweltbundesamt, Fachgebiet Emissionssituation (V 1.6), June 2022. URL: https://www.umweltbundesamt.de/sites/default/files/medien/479/publikationen/cc_28-2022_emissionsfaktoren-brennstoffe_bf.pdf.

[51] Mirko Grljušić, Vladimir Medica, and Gojmir Radica. *Calculation of Efficiencies of a Ship Power Plant Operating with Waste Heat Recovery through Combined Heat and Power Production*. In: Energies 8.5 (2015), pp. 4273–4299. ISSN: 1996-1073. DOI: 10.3390/en8054273. URL: https://www.mdpi.com/1996-1073/8/5/4273.

Appendix

Table 7: List of Further Data and their Sources

	Value	**Unit**	**Reference Year**	**Reference**
Chemical Parameters				
Heating Vale Iron	2.05	TWh/Mt	-	
Heating Value Hard Coal	8.06	kWh/kg	-	-
Weight Factor Iron Oxid	1.43		-	
General Cost Parameter			-	
Exchange \$/€	0.9	$\$ \rightarrow €$	04/2023	-
Inflation Rates (HICP)	[0.1,9.2]	%	-	[10, 11, 12]
Carrier Parameter				
Lower Heating Value VLSFO	$11.7\overline{2}$	TWh/Mt	-	[31, Sec. 4.6.2], [30]
Emission Rate VLSFO	3.188	t_{CO_2}/t_{VLSFO}	-	[31, Sec. 4.6.2]
Barge Parameter				
Lower Heating Value Diesel	11.94	TWh/Mt	-	-
Efficiency Diesel Engine	54.2	%	-	[51]
Emission Rate Diesel	3.165	t_{CO_2}/t_{Diesel}	-	[46, Tab. 10]
Power Diesel Engine	3264	kW	-	[38, Tab. 41]
Train Parameter				
Energy Consumption Train	0.0215	$kWh_{el}/(Nt \cdot km)$	-	[38, Tab. 30]
German Emission Line Electricity	100	g_{CO_2}/kWh_{el}	-	[44]

Table 8: Power Plants considered in the Case Study

	BNetzA power plant number	**Name of the power generation unit**	**Municipality**	**Year of Comissioning**	**Electricity Generation Capacity [MW]**	**Iron demand [t/a]**	**(Inland) Port**	**Railway Connection**	**Seaside Access**
1	BNA0019	Heizkraftwerk Altbach/Deizisau HKW 2 DT	Altbach	29.05.1997	336	1 547 183	x	x	
2	BNA0144	KW Hastedt Block 15	Bremen	16.12.1989	119	547 960	x		
3	BNA1949	Datteln 4	Datteln	30.05.2020	1 055	4 857 969	x		
4	BNA0216b	Walsum 10	Duisburg	20.12.2013	725	3 338 415	x	x	
5	BNA0518b	Rheinhafen-Dampfkraftwerk RDK 8	Karlsruhe	01.07.2014	834	3 840 328	x	x	
6	BNA1508	Trianel Kohlekraftwerk Lünen	Lünen	01.01.2013	735	3 384 462	x	x	
7	BNA0644	GKM Block 6	Mannheim	26.12.2005	255	1 174 201	x	x	
8	BNA0646b	GKM Block 9	Mannheim	02.05.2015	843	3 881 770	x	x	
9	BNA1674	Kraftwerk Wilhelmshaven Onyx	Wilhelmshaven	30.11.2015	731	3 366 043	x	x	x
10	BNA1558	Moorburg B	Hamburg	2015	800	3 683 768	x		x
11	BNA1673	Moorburg A	Hamburg	2015	800	3 683 768	x		x
12	BNA0413c	Westfalen E	Hamm-Uentrop	2014	764	3 516 617	x	x	
13	BNA0849	Kraftwerk Rostock Block A	Rostock	01.10.1994	514	2 366 821	x	x	x
14	BNA0402	HKW Tiefstack	Hamburg	01.04.1993	194	893 314	x	x	x
15	BNA0646a	GKM Block 8	Mannheim	05.04.1993	435	2 003 049	x	x	
16	BNA0377	Staudinger 5	Großkrotzenburg	01.01.1992	510	2 348 402	x	x	
17	BNA0420	GKH 1	Hannover	26.01.1989	136	626 241	x	x	
18	BNA0421	GKH 2	Hannover	21.06.1989	136	626 241	x	x	
19	BNA0999	Fenne HKV	Völklingen	30.11.1989	211	971 594		x	
20	BNA0450	Herne 4	Herne	25.07.1989	449	2 067 515	x	x	
21	BNA0087	HKW Reuter West Dampfturbine E	Berlin	01.08.1988	282	1 298 528	x	x	
22	BNA0216a	Walsum 9	Duisburg	10.06.1905	370	1 703 743	x	x	
23	BNA0793	Heyden 4	Petershagen	01.01.1987	875	4 029 121	x	x	
24	BNA0086	HKW Reuter West Dampfturbine D	Berlin	14.12.1987	282	1 298 528	x	x	
25	BNA1093	Kraftwerk Zolling	Zolling	01.01.1985	472	2 173 423		x	
				Σ	**12 863**	**59 229 001**			

Working Paper Series in Production and Energy

recent issues

Impressum

Karlsruher Institut für Technologie

Institut für Industriebetriebslehre und Industrielle Produktion (IIP)
Deutsch-Französisches Institut für Umweltforschung (DFIU)

Hertzstr. 16
D-76187 Karlsruhe

KIT – Universität des Landes Baden-Württemberg und
nationales Forschungszentrum in der Helmholtz-Gemeinschaft

Working Paper Series in Production and Energy
No. 70, April 2023

ISSN 2196-7296